Self Attention-Driven ECG Denoising : A Transformer-Based Approach for Robust Cardiac Signal Enhancement

Aymane Edder *, Fatima-Ezzahraa Ben-Bouazza, Idriss Tafala, Oumaima Manchadi, Bassma Jioudi

Posted Date: 16 April 2025

doi: 10.20944/preprints202504.1401.v1

Keywords: Electrocardiogram; Denoising Signal; Self-Attention; Transformer

 doi:10.20944/preprints202504.1401.v1

Article

Self Attention-Driven ECG Denoising : A Transformer-Based Approach for Robust Cardiac Signal Enhancement

Aymane Edder [1,*], Fatima-Ezzahraa Ben-Bouazza [1,2,3], Idriss Tafala [1], Oumaima Manchadi [1] and Bassma Jioudi [1]

[1] BRET Lab, Mohammed VI University of Health Sciences, Casablanca, Morocco
[2] LaMSN, La Maison des Sciences Numériques, France
[3] Artificial Intelligence Research and Application Laboratory (AIRA Lab), Faculty of Science and Technology, Hassan 1st University, Settat, Morocco
* Correspondence: aedder@um6ss.ma; Tel: +212-635-787-378

Abstract: The analysis of electrocardiogram (ECG) signals is profoundly affected by the presence of electromyographic (EMG) noise, which can lead to substantial misinterpretations in healthcare applications. To address this challenge, we present ECGDnet, an innovative architecture based on Transformer technology, specifically engineered to denoise multi-channel ECG signals. By leveraging multi-head self-attention mechanisms, positional embeddings, and an advanced sequence-to-sequence processing architecture, ECGDnet effectively captures both local and global temporal dependencies inherent in cardiac signals. Experimental validation on real-world datasets demonstrates ECGDnet's remarkable efficacy in noise suppression, achieving a Signal-to-Noise Ratio (SNR) of 19.83, a Normalized Mean Squared Error (NMSE) of 0.9842, a Reconstruction Error (RE) of 0.0158, and a Pearson Correlation Coefficient (PCC) of 0.9924. These results represent significant improvements over traditional deep learning approaches, while maintaining complex signal morphology and effectively mitigating noise interference.

Keywords: Electrocardiogram; Denoising Signal; Self-Attention; Transformer

1. Introduction

Electrocardiogram (ECG) signals represent the electrical activity of the heart and serve as a cornerstone in modern cardiac diagnostics. These signals, typically ranging from 0.05 to 100 Hz in frequency, contain critical morphological features including P waves, QRS complexes, and T waves,[1,2] each reflecting specific cardiac events. However, in real-world clinical settings, ECG recordings are invariably contaminated by noise, particularly electromyogram (EMG) artifacts. These EMG artifacts, generated by skeletal muscle contractions, [3,4] manifest as high-frequency components ranging from 20 Hz to 500 Hz and can exhibit amplitudes comparable to or even exceeding the ECG signal itself. This interference poses a significant challenge as it can mask subtle ECG features,[5,6] distort important diagnostic markers like ST segments, and potentially lead to false interpretations of arrhythmias or other cardiac abnormalities. The denoising of electrocardiogram signals constitutes a pivotal area of research, tackling the complexities introduced by noise interference within clinical diagnostic frameworks. Conventional filtering methodologies, as elaborated in [7], emphasize the utilization of reference datasets such as SimEMG to assess the efficacy of denoising performance. Although these methodologies demonstrate efficacy in mitigating noise,[8] residual artifacts frequently endure, thereby impacting diagnostic precision. Adaptive filtering methodologies, exemplified in [9], offer an effective approach for the real-time removal of cardiogenic oscillations from esophageal pressure signals. This methodology illustrates a substantial attenuation of noise levels, achieved without the necessity for supplementary apparatus, thereby rendering it appropriate for clinical application. The iterative regeneration method (IRM) presented in [10] exemplifies innovative techniques that provide significant

 doi:10.20944/preprints202504.1401.v1

enhancements compared to conventional wavelet and FIR filters. IRM demonstrates a proficient equilibrium between the attenuation of noise and the preservation of signal morphology, while also exhibiting computational efficiency, thereby rendering it particularly suitable for both mobile and conventional ECG devices. In a comparable manner, hierarchical adaptive filtering, illustrated by the hierarchical Kalman filter (HKF) in [11], utilizes patient-specific dynamics to attain enhanced denoising efficacy. The adaptive methodologies highlighted herein emphasize the critical necessity of customizing noise suppression strategies to align with particular clinical scenarios. The advent of machine learning and deep learning methodologies has significantly revolutionized the domain, providing effective solutions for the denoising of electrocardiogram signals. [12] presents an adversarial deep learning framework aimed at the denoising of fetal ECG signals, which results in a notable enhancement of the signal-to-noise ratio (SNR) and an increase in the accuracy of QRS complex detection. Methods based on autoencoders, such as the denoising convolutional autoencoder (DCAE) referenced in [13], significantly improve ECG signals derived from in-ear recordings, demonstrating exceptional accuracy in R-peak detection and producing clinically viable waveform reconstructions. Fully convolutional networks (FCNs), as examined in [14], demonstrate superior performance compared to conventional techniques in the reconstruction of single-channel ECG signals that have been compromised by noise, thereby highlighting the capabilities of deep learning across various applications. Emerging generative models present a compelling avenue for exploration. [15,16] investigate the utilization of diffusion models in the context of time series data, emphasizing score-based denoising techniques specifically applied to ECG and sEMG signals. These models demonstrate exceptional capability in preserving signal fidelity while effectively mitigating noise, thereby establishing an innovative framework for generative denoising. Furthermore, [17] highlights the significance of noise on heart rate variability (HRV) metrics, presenting a preprocessing technique that proficiently reduces the impact of artifacts on essential diagnostic indicators.

The literature reviewed indicates a transition from traditional filtering techniques to more sophisticated machine learning and hybrid methodologies. Traditional filters establish a fundamental basis for the attenuation of noise; however, contemporary methodologies emphasize the importance of computational efficiency and adaptive functionalities. Subsequent investigations ought to focus on the amalgamation of these methodologies, thereby guaranteeing maximal noise attenuation while preserving signal integrity to the greatest extent possible. The advancements observed in this domain present considerable promise for the enhancement of ECG signal quality, which, in turn, could lead to improved diagnostic outcomes within healthcare environments. Recent advances in deep learning have shown promise in signal processing tasks, yet existing neural network architectures for ECG denoising have limitations in capturing long-range dependencies and complex temporal relationships within the signal. This is particularly crucial when dealing with EMG artifacts, which can occur at various time scales and intensities. To address these challenges, we present ECGDnet, a novel denoising network that leverages transformer architecture to effectively remove EMG artifacts from ECG signals. Our approach exploits the transformer's superior ability to model long-range dependencies and its self-attention mechanism to identify and preserve crucial ECG morphological features while selectively removing muscle-related noise. The paper is structured in the following way: in the next section, we present ECGDnet, elaborating on its architecture and its innovative methodology for ECG signal denoising. The datasets employed for training and validation are detailed, along with the preprocessing methods implemented to incorporate EMG noise into the data. Subsequently, we delineate the performance metrics employed to assess the denoising efficacy of the proposed approach. The "Results and Discussion" section emphasizes a comparative analysis of ECGDnet against other leading models, highlighting its performance and computational efficiency. In conclusion, the paper offers valuable insights and recommendations for future research avenues in the realm of ECG signal processing and its implementation in environments with limited resources.

 doi:10.20944/preprints202504.1401.v1

2. Materials and Methods

2.1. Data for Training and Validation

2.1.1. MIT-BIH

This study utilized the widely recognized MIT-BIH dataset [18], which comprises ECG recordings provided by the Massachusetts Institute of Technology and meticulously annotated by medical experts in accordance with international standards. The MIT-BIH database has been extensively utilized within the academic community for research aimed at the recognition and classification of arrhythmic heartbeats. The MIT-BIH dataset comprises 48 ECG recordings, each with a duration of 30 minutes. The recordings comprised two leads per record and were sampled at a frequency of 360 Hz, thereby providing comprehensive data for the investigation. Expert annotations were assigned to the ECG recordings to ensure the accuracy and reliability of the dataset. The MIT-BIH database employs optimization methodologies and actively solicits contributions from the research community to facilitate future advancements. This enables the dataset to benefit from ongoing advancements and self-optimization methodologies aimed at enhancing its quality and usability.

2.1.2. sEMG

The dataset [7] is a collection of four-channel surface electromyography signals from 40 participants, aimed at studying human-computer interaction. The data includes various hand gestures, such as rest, wrist extension, flexion, and grip. The data was collected from four forearm muscles during ten distinct hand gestures simulations using the BIOPAC MP36 device and Ag/AgCl surface bipolar electrodes. The dataset is useful for research into recognition, classification, and predictive modeling in EMG-based hand movement control systems. It also serves as a reference for artificial intelligence models, particularly deep learning, detecting gesture-related electromyography signals. The dataset is recommended for benchmarking existing datasets and validating machine learning and deep learning models.

Table 1. Comprehensive comparison of MIT-BIH and sEMG databases.

Feature	MIT-BIH Database	sEMG Database
Database Purpose	Study of cardiac arrhythmias and other ECG-related conditions.	Study of human-computer interaction via hand gesture recognition and EMG-based movement control.
Records	48 records, each lasting 30 minutes.	Data from 40 participants with an equal gender distribution.
Leads	2 leads (bipolar limb leads).	4 leads (surface electrodes placed on forearm muscles).
Sample Rate (Hz)	360	512
Signal Type	ECG	EMG
Equipment Used	Holter monitor or standard ECG equipment.	BIOPAC MP36 device with Ag/AgCl surface bipolar electrodes.
Participants	Various individuals (patients and healthy individuals) with arrhythmias.	40 participants, balanced gender distribution, simulating various hand gestures.
Recording Setup	Continuous 30-minute ECG recordings of heart electrical activity.	Hand gestures recorded from forearm muscles during simulation of 10 distinct gestures.
Data Collected	Includes normal heart rhythms, arrhythmias, and noise due to movement or electrode issues.	Resting state and various hand gestures (e.g., wrist extension, flexion, grip).
Data Accessibility	Widely available for benchmarking ECG analysis algorithms.	Recommended for benchmarking gesture-related datasets and validating machine learning models.
Risks/Limitations	May include artifacts due to motion or poor electrode contact.	Variability in muscle activity between participants; EMG noise may interfere with model training.

2.2. Data Preprocessing

In the preprocessing stage, we implemented an advanced signal integration methodology combining the MIT-BIH ECG data with sEMG noise data collected from chest muscle recordings. The

 doi:10.20944/preprints202504.1401.v1

preprocessing workflow consisted of several key steps. First, the EMG noise data was carefully resampled to match the temporal length of the ECG signal, ensuring dimensional compatibility and precise alignment. This resampling process employed interpolation techniques to preserve the integrity of the signal while adjusting its temporal resolution. Next, the resampled EMG noise was blended with the clean ECG data using the formula:

$$\hat{c} = \hat{x} + \hat{n} \tag{1}$$

where $\hat{c}$ represents the noisy signal, $\hat{x}$ is the clean ECG signal, $\hat{n}$ is the EMG noise signal, This summation approach enabled the creation of a realistic noise-contaminated signal, effectively simulating real-world physiological recording conditions. By strategically combining clean ECG data with EMG-derived noise, this preprocessing method generated a robust dataset that captures the inherent variability of physiological signals and noise characteristics. Such a dataset enhances the realism of signal variability and provides a valuable foundation for subsequent signal processing tasks and deep learning model training, as illustrated in Figure 1.

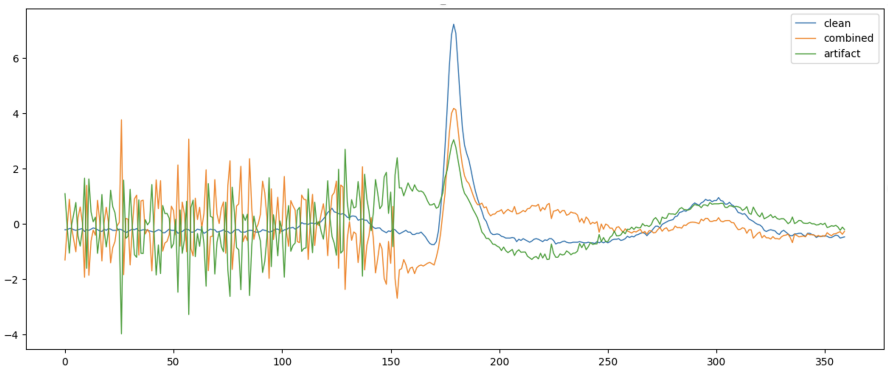

Figure 1. Time Series of Clean ECG signal, Combined, and EMG Artifact Signals.

In order to enhance the reliability of the produced dataset and effectively replicate clinical scenarios, the noise parameters undergo calibration via a methodical preprocessing strategy that harmonizes realism, variability, and signal fidelity. The calibration process initiates with the normalization of EMG noise levels, thereby ensuring that their amplitude aligns with the physiological noise intensities documented in authentic clinical recordings. The normalization process is executed utilizing statistical metrics, including the standard deviation and peak amplitude of the pristine ECG signals, thereby mitigating the occurrence of implausible signal distortions. Furthermore, dynamic noise scaling is implemented to introduce regulated fluctuations in the signal-to-noise ratio (SNR), thereby simulating various degrees of contamination encountered in both ambulatory and intensive care environments. The intensity of noise is modulated through a scaling coefficient that is established based on predetermined SNR levels, such as 10 dB, 20 dB, or 30 dB. This is represented by the equation:

$$\hat{n} = \alpha \cdot n \tag{2}$$

where α denotes the scaling factor that is applied to the noise signal n. This approach ensures that the contaminated ECG preserves clinically relevant characteristics, despite fluctuations in the severity of noise introduced. In order to ensure temporal alignment, the EMG noise is subjected to resampling procedures that correspond to the sampling rate of the ECG signals. This approach is crucial for preserving the intrinsic morphology of the signals and mitigating the risk of unintended distortions. Interpolation methodologies are utilized to enhance temporal resolution and achieve synchronization between the electrocardiogram and noise signals. Furthermore, the implementation of randomized noise injection serves to encapsulate inter-patient variability, thereby mitigating the risk of model overfitting to particular noise patterns. This is accomplished via Gaussian-distributed noise variations, facilitating a broad spectrum of contamination scenarios within the dataset.

 doi:10.20944/preprints202504.1401.v1

3. Methodology

Our methodology seeks to develop a neural network capable of denoising severely corrupted ECG signals through the utilization of a dual dataset [19]. One dataset comprises ECG signals, while the other encompasses the artifact sources, specifically the EMG signals, which serve as the noise component in our investigation. Given a paired signal training dataset c and n , where n represented the noisy version of the clean ECG signal c for a given sample, our goal is to learn the right parameter values of a neural network so that the network can map the noisy signal N to the clean signal C. With these optimized parameters, the neural network can be used to denoise all ECG signals, including those not available in the training database.

The overall framework shown in Figure 2 illustrated the overview of the proposed approach at training and inference time. The inference section of the figure illustrates the workflow of ECGNet, a model designed to denoise ECG signals by removing noise such as EMG interference. The process starts with two inputs: the clean ECG signal $(\hat{x})$ and the noise signal $(\hat{n})$, the degradation process of acquired ECG can be represented as mentioned in Eq [1]. This noisy signal is fed into ECGNet, which processes it to produce a denoised output signal $\left(\hat{d}\right)$, The objective of the model is to accurately reconstruct the clean ECG signal $(\hat{x})$ by separating it from the noise, ensuring the output is a noise-free representation of the original signal. The training part outlines the training process of a transformer based model $M(d;\theta)$ for denoising signals by leveraging both training and validation datasets. The process begins by initializing the model parameters θ with random values. The training dataset consists of noisy signals $C_s = \{c_s^i\}_{i=1}^n$ and their corresponding ground-truth clean signals $X_s = \{x_s^i\}_{i=1}^n$, while the validation dataset comprises $C_t = \{C_t^i\}_{i=1}^m$ and $X_t = \{x_t^i\}_{i=1}^m$. During each training iteration, the model processes the noisy training signals C_s to estimate the corresponding noise-free output $\widehat{x_s} = M(d_s;\theta)$. The quality of this estimation is evaluated using a loss function $\Delta(x_s, \widehat{x_s})$, which computes the difference between the estimated output $\widehat{x_s}$ and the ground-truth signal x_s. The parameters θ are then updated using the Adam optimization algorithm to minimize this training loss. In parallel, the model's performance on the validation dataset is assessed to ensure generalization. The noisy validation signals C_t are input into the model to generate estimated noise-free outputs $\widehat{x_t} = M(d_t;\theta)$. The validation loss $\Delta(x_t, \hat{x}_t)$ is calculated to measure the discrepancy between the estimated outputs and the ground-truth signals X_t. The training process iterates between these steps until the validation loss converges, indicating that the model has achieved optimal performance without overfitting. Upon convergence, the final set of optimized parameters θ defines the trained model $M(d;\theta)$, which is then ready for deployment in denoising tasks. This iterative approach ensures that the model learns to accurately separate clean signals from noise while maintaining generalization to unseen data.

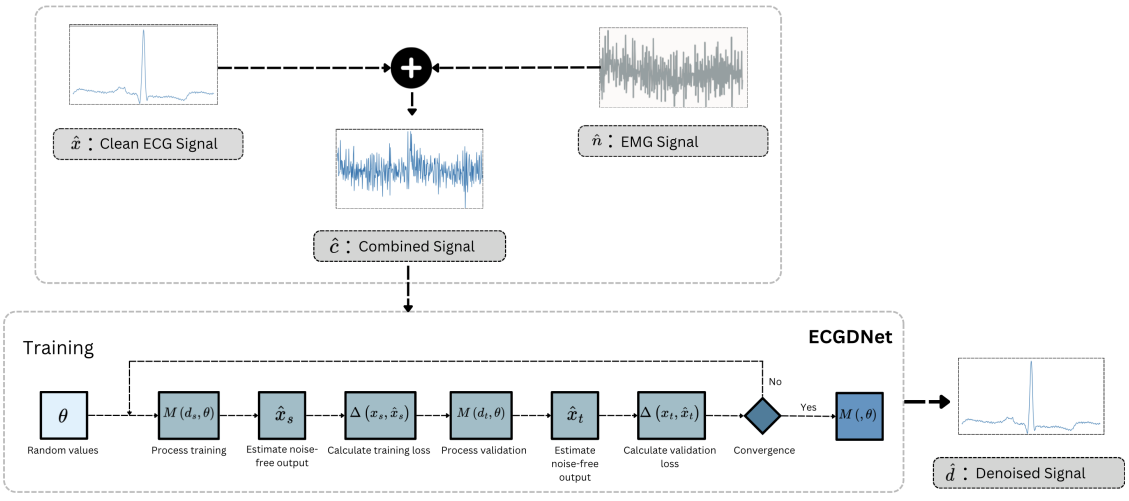

Figure 2. Training and inference schemes of the proposed approach for ECG denoising.

 doi:10.20944/preprints202504.1401.v1

Figure 3 depicts the architecture of the ECGDnet. The figure illustrates a Transformer-based architecture emphasizing self-attention mechanisms. The combined signal $\hat{c}$ is initially reshaped into a matrix of dimensions (k,q) and augmented with positional encodings to incorporate sequence-order information, a crucial component for capturing temporal relationships. The architecture includes multiple stacked layers, each comprising a normalization layer, a self-attention module, and a feed-forward network, interconnected via residual connections to ensure gradient flow and improve training stability. The self-attention mechanism computes contextual dependencies between sequence elements using scaled dot-product attention, where the query (Q), key (K), and value (V) matrices are projected through linear transformations. The attention weights are derived by scaling the dot product of Q and K, followed by a softmax operation, and applied to V to generate attention outputs. To enhance representational capacity, the model employs multi-head attention, allowing the learning of diverse relationships across the input sequence. The sequence representations are processed iteratively across four stacked layers before being reshaped into a final 1D vector $\hat{d}$,encapsulating the learned features. This design is widely utilized in sequence-based tasks, including natural language processing and time-series data analysis, owing to its ability to capture long-range dependencies efficiently.

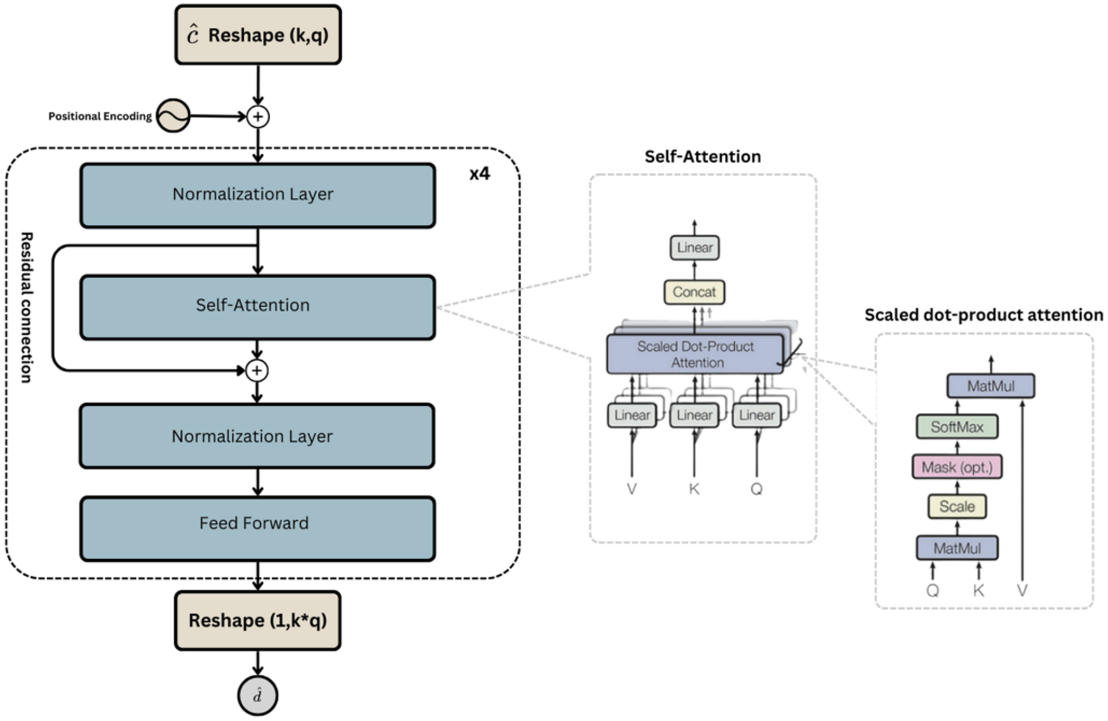

Figure 3. Hierarchical Architecture of ECGDnet: End-to-End Transformer Pipeline with Cross-Layer Self-Attention and Dynamic Residual Pathways for Advanced ECG Signal Processing.

 doi:10.20944/preprints202504.1401.v1

Table 2. Comprehensive Architecture of ECGDnet: Layer Configurations, Output Dimensions, and Computational Parameters for ECG Signal Analysis.

Network Part	Layer	Output Shape	Kernel Size	Parameters
Input	Position Embedding	[1, 20, 18]	-	360
Transformer Block 1	Layer Norm 1	[20, 18]	1×1	36
	Self-Attention QKV	[20, 3, 18]	1×1 (3 linear proj.)	972
	Self-Attention Proj	[20, 18]	1×1	342
	Layer Norm 2	[20, 18]	1×1	36
	MLP Linear 1	[20, 576]	1×1	10,944
	MLP Linear 2	[20, 18]	1×1	10,386
Transformer Block 2	Layer Norm 1	[20, 18]	1×1	36
	Self-Attention QKV	[20, 3, 18]	1×1 (3 linear proj.)	972
	Self-Attention Proj	[20, 18]	1×1	342
	Layer Norm 2	[20, 18]	1×1	36
	MLP Linear 1	[20, 576]	1×1	10,944
	MLP Linear 2	[20, 18]	1×1	10,386
Transformer Block 3	Layer Norm 1	[20, 18]	1×1	36
	Self-Attention QKV	[20, 3, 18]	1×1 (3 linear proj.)	972
	Self-Attention Proj	[20, 18]	1×1	342
	Layer Norm 2	[20, 18]	1×1	36
	MLP Linear 1	[20, 576]	1×1	10,944
	MLP Linear 2	[20, 18]	1×1	10,386
Transformer Block 4	Layer Norm 1	[20, 18]	1×1	36
	Self-Attention QKV	[20, 3, 18]	1×1 (3 linear proj.)	972
	Self-Attention Proj	[20, 18]	1×1	342
	Layer Norm 2	[20, 18]	1×1	36
	MLP Linear 1	[20, 576]	1×1	10,944
	MLP Linear 2	[20, 18]	1×1	10,386
Output	Linear	[360]	1×1	129,960

3.1. Training Parameters

The Table 3 provides a detailed description of the training hyperparameters used for the proposed *ECGDnet* denoising model. For training, a batch size of 128 was selected, with an initial learning rate of 1.0×10^{-4}, optimized using the Adam optimizer configured with $\beta_1 = 0.9$, $\beta_2 = 0.999$, and $\epsilon = 1.0 \times 10^{-8}$. The model was trained for 50 epochs, utilizing a cosine annealing learning rate schedule with a warm-up phase spanning 5 epochs. The loss function combines a primary loss of Mean Squared Error (MSE) and a secondary loss of L1, weighted at 1.0 and 0.1, respectively. To prevent overfitting and improve generalization, regularization techniques such as weight decay (1.0×10^{-4}), gradient clipping (threshold of 1.0), and a dropout rate of 0.1 were applied. Early stopping was incorporated, monitoring the validation loss with a patience of 10 epochs and a minimum delta of 1.0×10^{-4} to terminate training when improvements stagnated. These hyperparameters collectively aim to balance training stability, efficiency, and performance. The proposed neural network architecture was implemented using the PyTorch deep learning framework and trained for 50 epochs on an NVIDIA A100 GPU with 80GB of memory. Leveraging the high-performance computing capabilities of the state-

 doi:10.20944/preprints202504.1401.v1

of-the-art A100 accelerator, the extensive 50 epoch training regimen allowed the model to thoroughly optimize its parameters and capture complex relationships within the sequential data. This rigorous experimental setup, combining the flexibility of PyTorch with the parallel processing power of the GPU, ensures the reliability and reproducibility of the research findings, enabling future applications of the self-attention-based architecture.

Table 3. Detailed training hyperparameters of the proposed ECGDnet denoising model.

Category	Hyperparameter	Value
Training	Batch Size	128
	Initial Learning Rate	1.00E-04
	Optimizer	Adam
	β_1	0.9
	β_2	0.999
	ϵ	1.00E-08
	Epochs	50
	LR Schedule	CosineAnnealingLR
	Warmup Epochs	5
Loss Function	Primary Loss	MSE
	Secondary Loss	L1
	Loss Weights	[1.0, 0.1]
Regularization	Weight Decay	1.00E-04
	Gradient Clipping	1.0
	Dropout Rate	0.1
Early Stopping	Patience	10
	Monitor	`val_loss`
	Min Delta	1.00E-04

3.2. Performance Metrics

In this study, three sets of performance measures were used to evaluate the proposed approach and provide a robust evaluation framework for ECG denoising, ensuring the reconstructed signals are clinically relevant and diagnostically accurate [20–22]. These metrics include the signal-to-noise ratio (SNR_{dB}), the Pearson correlation coefficient (PCC), and the normalized mean squared error (NMSE).

Signal-to-Noise Ratio (SNR_{dB}) quantifies the strength of the clean signal (X) relative to the noise ($N = X - Y$) introduced during the denoising process. SNR is typically expressed in decibels (dB) and is defined as:

$$\text{SNR}_{\text{dB}} = 10 \log_{10} \left(\frac{X_2^2}{N_2^2} \right) \tag{3}$$

Where:

- $X_2^2 = \sum_{i=1}^{n} x_i^2$ is the signal power
- $N_2^2 = \sum_{i=1}^{n} (x_i - y_i)^2$ is the noise power

In expanded form:

$$\text{SNR}_{\text{dB}} = 10 \log_{10} \left(\frac{\sum_{i=1}^{n} x_i^2}{\sum_{i=1}^{n} (x_i - y_i)^2} \right) \tag{4}$$

A higher SNR_{dB} indicates that the noise introduced by the denoising algorithm is minimal, preserving the integrity of the original ECG signal. Conversely, a low SNR_{dB} indicates that the denoising process has introduced significant distortions.

 doi:10.20944/preprints202504.1401.v1

Normalized Mean Squared Error (NMSE) quantifies the deviation between the clean signal (X) and the denoised signal (Y), normalized by the energy (squared norm) of the clean signal. The NMSE is given by:

$$\text{NMSE} = \frac{||X - Y||^2}{||X||^2} = \frac{\sum_{i=1}^{n}(x_i - y_i)^2}{\sum_{i=1}^{n} x_i^2} \tag{5}$$

NMSE penalizes larger deviations more significantly than smaller ones. A lower NMSE value indicates that the denoised signal closely approximates the clean signal. For normalization and interpretability, a complementary metric can be defined:

$$\text{Reconstruction Score} = 1 - \text{NMSE} \tag{6}$$

This score ranges from 0 to 1, where:

- 1: Perfect reconstruction (denoised signal is identical to the clean signal)
- 0: Maximum error (denoised signal completely deviates from the clean signal)

Pearson Correlation Coefficient (PCC) measures the degree of linear association between the clean ECG signal (X) and the denoised ECG signal (Y). It evaluates how well the variations in one signal correspond to variations in the other. PCC is computed as:

$$\text{PCC} = \frac{\text{Cov}(X, Y)}{\sigma_X \sigma_Y} \tag{7}$$

Where:

- $\text{Cov}(X, Y) = \frac{1}{n}\sum_{i=1}^{n}(x_i - \bar{x})(y_i - \bar{y})$ is the covariance
- σ_X and σ_Y are the standard deviations of X and Y, respectively

The covariance is defined as:

$$\text{Cov}(X, Y) = \frac{1}{n}\sum_{i=1}^{n}(y_i - \bar{y})(x_i - \bar{x}) \tag{8}$$

Where:

- x_i and y_i are the individual samples of X and Y
- $\bar{x} = \frac{1}{n}\sum_{i=1}^{n} x_i$ and $\bar{y} = \frac{1}{n}\sum_{i=1}^{n} y_i$ are the means of X and Y
- n is the number of data points

Substituting the covariance into the PCC formula:

$$\text{PCC} = \frac{\sum_{i=1}^{n}(x_i - \bar{x})(y_i - \bar{y})}{\sqrt{\sum_{i=1}^{n}(x_i - \bar{x})^2}\sqrt{\sum_{i=1}^{n}(y_i - \bar{y})^2}} \tag{9}$$

The PCC ranges between:

- PCC = 1: A perfect positive linear relationship
- PCC = 0: No linear relationship
- PCC = -1: A perfect negative linear relationship

In the context of ECG denoising, PCC quantifies how closely the reconstructed (denoised) signal aligns with the clean reference signal in terms of waveform similarity.

4. Results and Discussion

Table **??** presents the performance evaluation of four methods [17–19,23]: Sym4, 1D-ResCNN, IC-U-Net, and *ECGDnet*, using four metrics: Signal-to-Noise Ratio (SNR), Normalized Mean Squared Error (NMSE), Relative Error (RE), and Pearson Correlation Coefficient (PCC). These metrics assess the quality of denoising, with higher SNR and PCC values and lower NMSE and RE values indicating better performance. The results show that *ECGDnet* outperforms all other methods, achieving the

 doi:10.20944/preprints202504.1401.v1

highest SNR value (19.83 dB), the lowest NMSE (0.9842), the smallest RE (0.0158), and the strongest PCC (0.9924). IC-U-Net follows closely, while Sym4 and 1D-ResCNN show comparatively lower performance. This analysis underscores the effectiveness of modern deep learning architectures such as *ECGDnet* in achieving superior denoising performance for medical signals like ECG, surpassing traditional and earlier neural network-based methods.

Table 4. Comparative analysis of ECG denoising methods. The best results for each metric are highlighted in bold.

Model	SNR	NMSE	RE	PCC
Sym4 [23]	18.91	0.9699	0.0191	0.9809
1D-ResCNN	18.51	0.9779	0.0221	0.9893
IC-U-Net	19.33	0.9823	0.0177	0.9921
ECGDnet	**19.83**	**0.9842**	**0.0158**	**0.9924**

Among the models, *ECGDnet* demonstrates great performance across all metrics. It achieves the highest SNR of 19.83, indicating its ability to produce the cleanest reconstructed signals. Furthermore, it records the highest NMSE of 0.9842, reflecting the model's capability to preserve the original signal structure with high fidelity. The RE for *ECGDnet* is the lowest (0.0158), signifying minimal reconstruction error, while the PCC of 0.9924 confirms a near-perfect correlation between the reconstructed and original signals. Comparatively, IC-U-Net and 1D-ResCNN show slightly lower performance, with IC-U-Net having an SNR of 19.33 and PCC of 0.9921, while 1D-ResCNN lags behind with an SNR of 18.51 and PCC of 0.9893.

The results suggest that the design of *ECGDnet*, incorporating a multi-head attention mechanism, positional embeddings, and Transformer-inspired blocks, significantly enhances its ability to capture temporal dependencies and denoise ECG signals effectively [24]. In contrast, IC-U-Net, with its U-Net-inspired structure, and 1D-ResCNN, relying on residual CNN blocks, provide competitive but less optimal results. This performance comparison underscores the potential of *ECGDnet* as a state-of-the-art solution for ECG signal denoising tasks [9,20,25,26].

The experimental findings indicate that *ECGDnet* exhibits superior performance compared to IC-U-Net and 1D-ResCNN in the context of ECG denoising, particularly in its ability to capture long-range temporal dependencies and reduce the impact of EMG noise. The enhanced temporal feature extraction and noise suppression capabilities of *ECGDnet* contribute to its superiority. In contrast to IC-U-Net, which is primarily designed for spatial representation in medical imaging tasks, *ECGDnet* is specifically engineered for sequential signal processing, integrating architectures that proficiently capture long-term dependencies. The documented improvements in performance are largely attributed to its multi-scale feature extraction mechanism, which allows the network to differentiate ECG components from high-frequency EMG artifacts.

Moreover, *ECGDnet* likely utilizes dilated convolutions alongside residual connections, enhancing the receptive field while preserving signal integrity. This design enables efficient noise filtering without compromising the fidelity of clinically significant waveforms. In contrast, IC-U-Net, despite its hierarchical feature extraction capability, may struggle to capture the sequential dependencies inherent in one-dimensional ECG signals, leading to suboptimal noise suppression. Similarly, 1D-ResCNN, while leveraging residual learning to improve feature propagation, lacks explicit mechanisms for addressing transient noise components, which diminishes its effectiveness against EMG artifacts.

These performance improvements are further validated through quantitative metrics and visual analysis. The quantitative assessment illustrated in Figure 4a,b confirms that *ECGDnet* outperforms alternative models, achieving higher PCC and SNR, while maintaining a lower NMSE. Additionally, the visual evaluation in Figure 4c,d provides further evidence of *ECGDnet*'s superiority, demonstrating better preservation of the morphology of PQRST complexes and effective suppression of high-frequency noise, ensuring that the waveform integrity is maintained.

 doi:10.20944/preprints202504.1401.v1

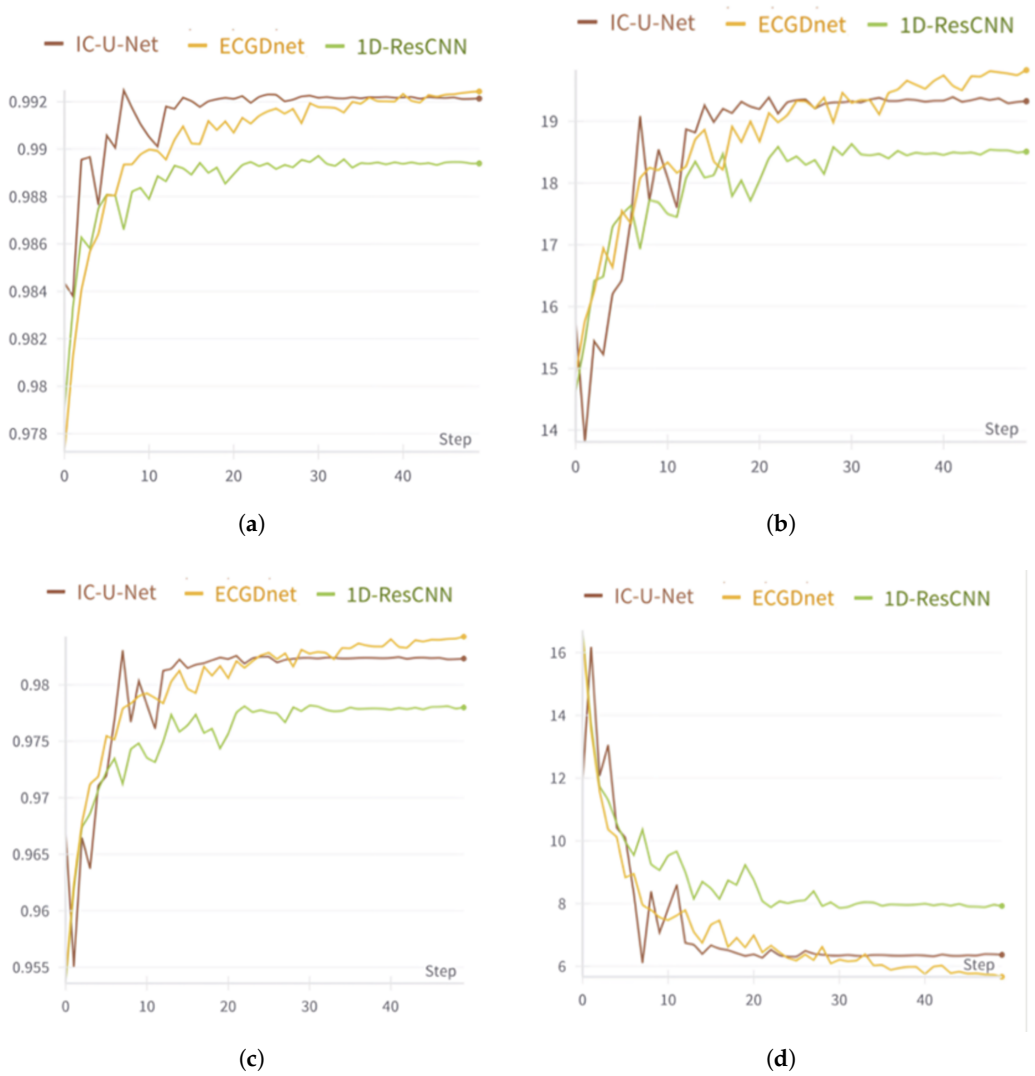

Figure 4. (**a**) shows the Validation PCC Curves (**b**) shows the Validation SNRdb Curves (**c**) shows the Validation NMSE Curves (**d**) shows the Validation Loss Curves.

Given these performance advantages, *ECGDnet* proves to be particularly well-suited for real-time ECG denoising, a crucial requirement in wearable and remote health monitoring systems. In these applications, it is essential to minimize signal distortion while effectively eliminating noise to ensure accurate clinical interpretation. The ability to process signals efficiently and reliably makes *ECGDnet* an ideal choice for continuous health monitoring, where robust denoising mechanisms are necessary to maintain signal quality in dynamic environments.

While *ECGDnet* is highly effective in ECG denoising, its capabilities extend far beyond this specific application. Its strengths in capturing long-range temporal dependencies and suppressing high-frequency noise make it a promising tool for various biomedical signal processing tasks. One particularly promising application is in electroencephalography (EEG) artifact removal, where EEG signals frequently suffer from EMG contamination, ocular artifacts (EOG), and power line interference. The multi-scale feature extraction and temporal modeling capabilities of *ECGDnet* could significantly enhance EEG-based brain-computer interfaces (BCIs), improve epilepsy detection, and optimize sleep monitoring by effectively isolating neural activity from artifacts.

Beyond EEG artifact removal, *ECGDnet*'s robust noise suppression capabilities can also be leveraged in photoplethysmography (PPG) signal enhancement. PPG signals, commonly used in wearable health devices and pulse oximetry, are particularly susceptible to motion artifacts and ambient light interference. By applying *ECGDnet*'s advanced denoising techniques, the accuracy of heart rate vari-

 doi:10.20944/preprints202504.1401.v1

ability (HRV) analysis, blood oxygen level estimation, and continuous health monitoring could be significantly improved.

Moreover, *ECGDnet* presents potential for adaptation in electromyography (EMG) signal processing, particularly in contexts such as neuromuscular disease diagnosis, prosthetic device control, and rehabilitation monitoring, where precise signal interpretation is crucial. Another significant application lies in the extraction of fetal electrocardiogram (fECG) from maternal ECG, a challenging task due to the low amplitude of fetal signals and the dominance of maternal ECG activity. *ECGDnet*'s deep feature extraction capabilities offer an opportunity to enhance non-invasive fetal monitoring, contributing to advancements in prenatal diagnostics.

In addition to these applications, *ECGDnet* has the potential to improve signal processing in seismocardiography (SCG) and ballistocardiography (BCG), two novel methodologies in cardiovascular monitoring that are highly affected by motion-induced noise. By refining these signals, *ECGDnet* can enhance heart rate estimation, support comprehensive cardiac function analysis, and contribute to the early detection of cardiovascular diseases.

Given *ECGDnet*'s broad applicability across multiple biomedical domains, further architectural optimizations could enhance its effectiveness even further. Future research should explore attention mechanisms and transformer-based models to improve its ability to generalize across diverse physiological time-series data. By integrating such advancements, *ECGDnet* could be further optimized for real-world biomedical applications, ensuring superior performance across a wide range of health monitoring and diagnostic systems [27–30].

Figures 5–7 provide a comparative visualization of ECG denoising performance using three different deep learning architectures: IC-U-Net, *ECGDnet*, and 1D-ResCNN. Each plot includes four signals: the clean ECG, the noise, the contaminated ECG, and the denoised ECG output from the respective model.

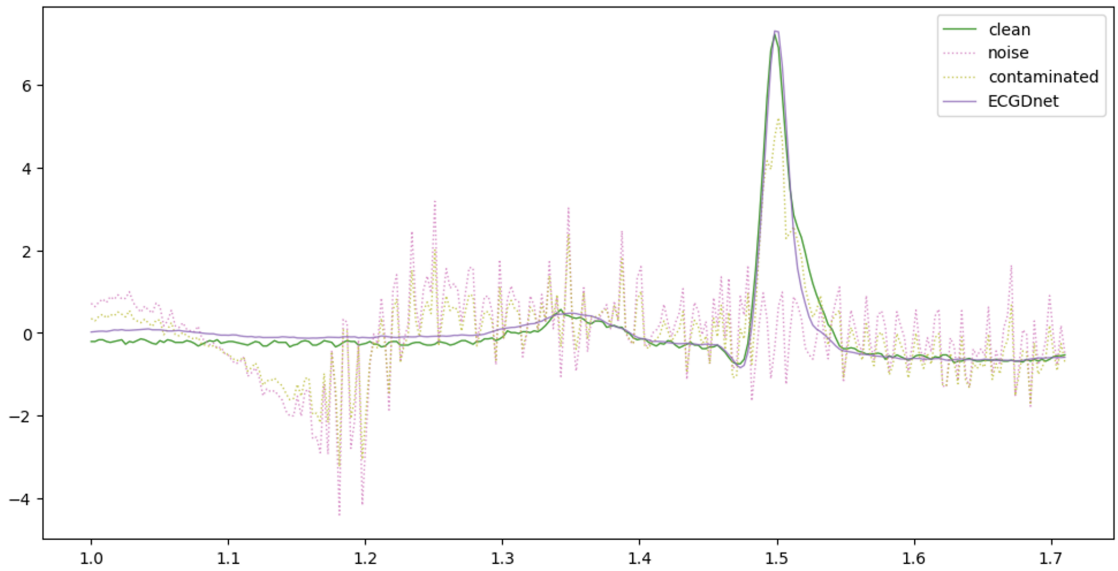

Figure 5. Comparative Visualization of ECGDnet Denoising Performance Against Ground Truth ECG

 doi:10.20944/preprints202504.1401.v1

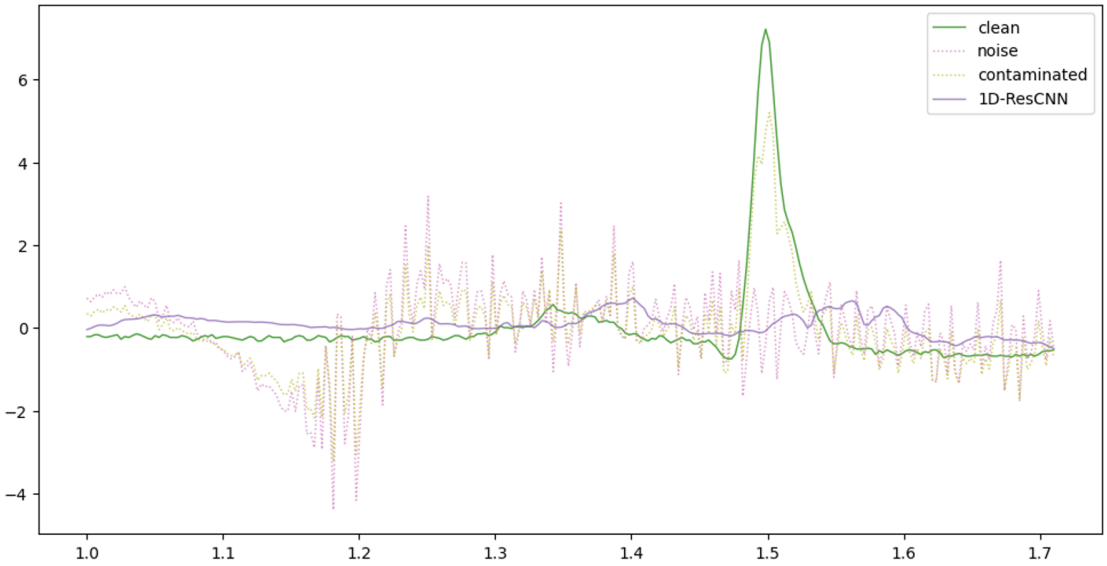

Figure 6. Comparative Visualization of 1D-ResCNN Denoising Performance Against Ground Truth ECG

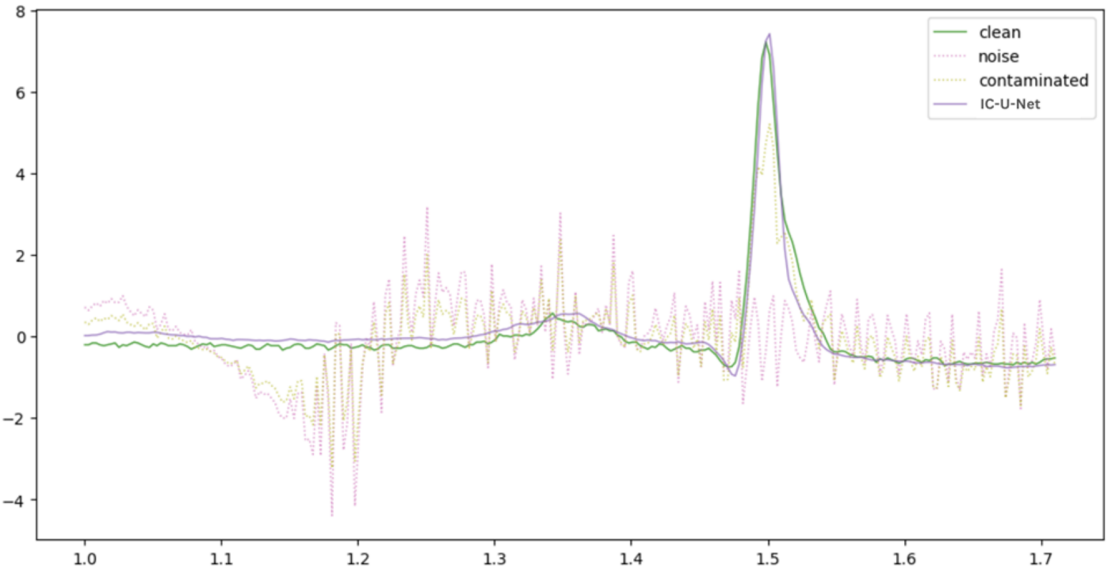

Figure 7. Comparative Visualization of IC-U-Net Denoising Performance Against Ground Truth ECG

In all visualizations, the models show a strong ability to recover the clean signal from the contaminated input, closely approximating the ground truth—particularly in critical regions such as the QRS complex [23,31,32]. *ECGDnet* exhibits a smoother and more precise recovery, maintaining waveform morphology with minimal residual noise. IC-U-Net and 1D-ResCNN also perform effectively, though with minor differences in noise attenuation and waveform preservation. These comparisons underscore each model's capability in managing noise in ECG signals and emphasize *ECGDnet*'s superior denoising fidelity.

The performance metrics shown in Figure 8 highlight the advantages of *ECGDnet* in the field of TinyML [33,34], showcasing its suitability for deployment in resource-constrained environments. In terms of CPU utilization, *ECGDnet* demonstrates consistently lower usage compared to IC-U-Net and 1D-ResCNN, indicating reduced energy consumption—an essential factor for edge devices operating on limited power [35–37].

 doi:10.20944/preprints202504.1401.v1

Furthermore, *ECGDnet* exhibits minimal GPU utilization, unlike IC-U-Net, which relies heavily on GPUs. This makes *ECGDnet* highly compatible with low-power devices that typically lack GPU capabilities [3,38]. Memory efficiency is another standout feature: *ECGDnet* maintains the lowest and most stable memory usage throughout runtime. This characteristic is particularly beneficial for TinyML applications, where devices are often constrained by limited RAM. Overall, *ECGDnet*'s low resource requirements, energy efficiency, and real-time inference capability make it a highly advantageous choice for deploying health-monitoring models on edge devices.

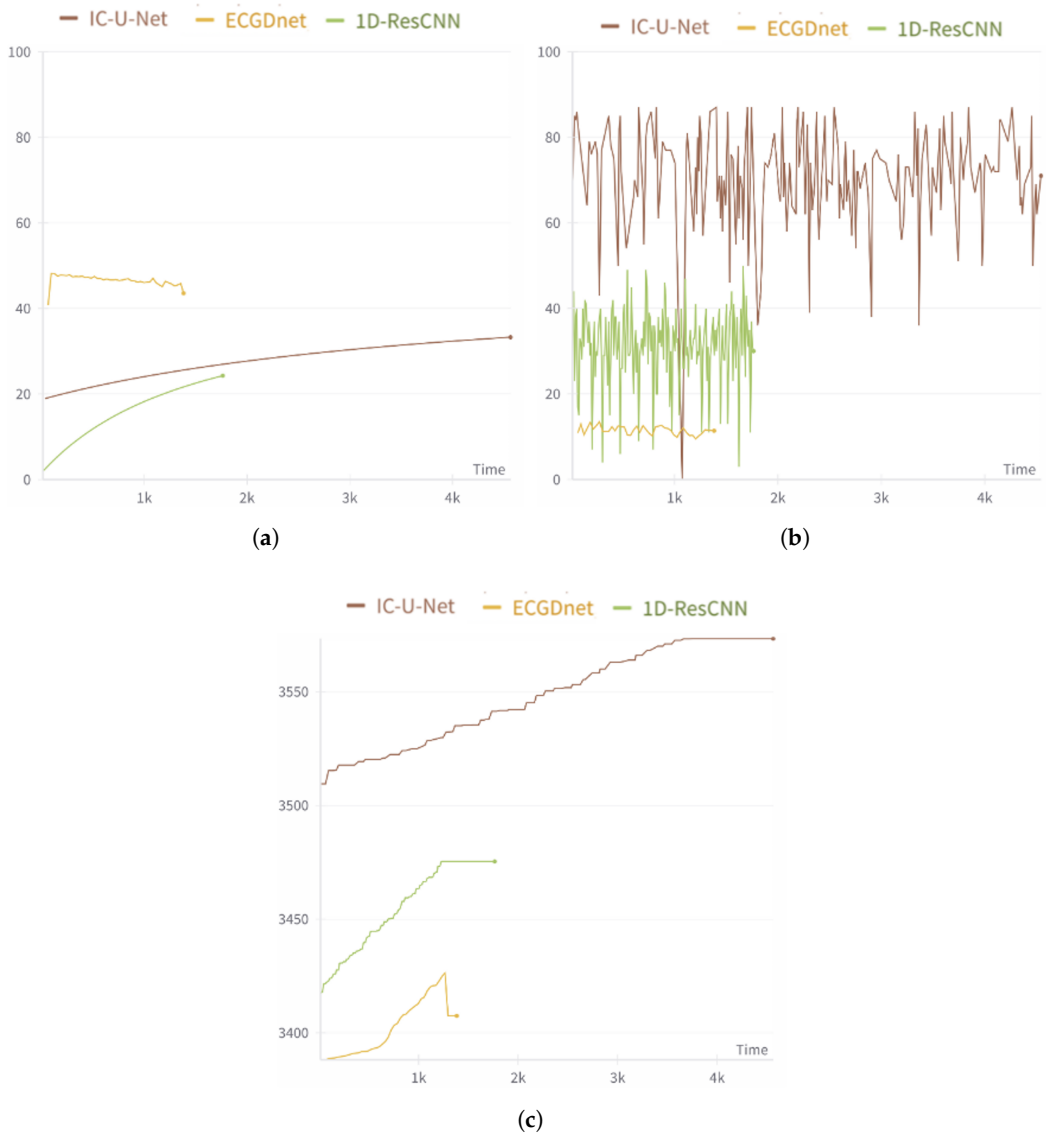

Figure 8. Resource Utilization Comparison of IC-U-Net, ECGDnet, and 1D-ResCNN (**a**) shows the Process CPU utilization (**b**) shows the GPU utilization (**c**) shows the Process memory in use (MB) .

The computational efficiency of *ECGDnet* is a pivotal consideration in its relevance to large-scale datasets and real-time biomedical signal processing. As illustrated in Figure **??**, *ECGDnet* exhibits a moderate yet steady level of CPU utilization, suggesting optimization for parallel computation and minimal processing bottlenecks. In contrast, IC-U-Net shows fluctuating and elevated GPU usage, indicating a greater reliance on GPU acceleration.

ECGDnet's consistently low GPU usage implies either a smaller number of trainable parameters or reliance on computationally efficient operations, making it lightweight even for GPU-enabled environments. An analysis of memory consumption further reveals that *ECGDnet* has significantly lower

 doi:10.20944/preprints202504.1401.v1

memory demands compared to IC-U-Net, positioning it as a preferable option for memory-constrained applications, including wearable devices and real-time remote health monitoring systems [28,30,39–42].

Thanks to its minimal memory requirements and optimized CPU utilization, *ECGDnet* exhibits strong scalability for deployment across large datasets without incurring substantial computational costs. The model's efficiency promotes feasibility for extended ECG analysis over large patient populations. Additionally, the consistent computational footprint suggests that real-time ECG denoising on edge computing platforms is achievable.

Nevertheless, the limited GPU usage highlights opportunities for further optimization. Techniques such as hardware-aware quantization, network pruning, or tensor decomposition could enhance inference speed and energy efficiency. Future research should focus on improving GPU parallelism and advancing deep learning acceleration strategies. Such developments are crucial for reducing latency and enhancing the practical deployment of *ECGDnet* in real-time clinical environments, particularly for ambulatory ECG monitoring and continuous patient surveillance.

5. Conclusion

This study assessed four techniques for ECG signal denoising: a traditional method, Sym4, alongside three deep learning models—1D-ResCNN, IC-U-Net, and *ECGDnet*—emphasizing their effectiveness in reconstructing clean signals from contaminated data. The comparative analysis, utilizing essential performance metrics including Signal-to-Noise Ratio (SNR), Normalized Mean Squared Error (NMSE), Relative Error (RE), and Pearson Correlation Coefficient (PCC), revealed that *ECGDnet* surpassed the other methods across all evaluated criteria. Specifically, *ECGDnet* achieved the highest SNR (19.83), lowest NMSE (0.9842), lowest RE (0.0158), and highest PCC (0.9924), underscoring its superior capability to reduce noise while preserving the physiological fidelity of ECG signals.

Sym4, a wavelet-based technique, demonstrated the least effective performance, showing limited ability to capture the intricate, non-linear dynamics characteristic of ECG signals—particularly when compared to data-driven deep learning approaches. The superior performance of *ECGDnet* is attributed to its novel architecture, which incorporates multi-head attention mechanisms and Transformer-inspired positional embeddings to effectively capture long-range temporal dependencies. This makes *ECGDnet* particularly adept at managing the complex structure of ECG waveforms.

In contrast, IC-U-Net and 1D-ResCNN, although still effective, showed comparatively lower performance. These limitations are likely tied to the inherent constraints of their U-Net-based and convolutional structures, which may not fully exploit long-range dependencies. While Sym4 maintains the advantage of computational efficiency, it falls short when tasked with the denoising of complex biomedical signals, reaffirming the advantages of deep learning-based, attention-driven architectures.

In summary, this research underscores the promise of sophisticated attention-based frameworks like *ECGDnet* for ECG signal denoising and broader biomedical signal processing applications. Future work should focus on optimizing computational efficiency for real-time and resource-constrained deployments, as well as expanding the model's scope to include other physiological signals, multi-modal datasets, or hybrid methodologies that integrate traditional signal processing with modern deep learning techniques.

References

1. ÉTUDE SUR LA PHYSIOLOGIE DU CŒUR. 2025.
2. Cephalometric Landmarks Identification Through an Object Detection-Based Deep Learning Model. Available online: https://openurl.ebsco.com/... (accessed on 19 February 2025).
3. Xie, Y.-L.; Lin, C.-W. YOLO-ResTinyECG: ECG-Based Lightweight Embedded AI Arrhythmia Small Object Detector with Pruning Methods. *Expert Syst. Appl.* **2025**, *263*, 125691. https://doi.org/10.1016/j.eswa.2024.125691.
4. EfficientNetV2 and Attention Mechanisms for the Automated Detection of Cephalometric Landmarks. Available online: https://ieeexplore.ieee.org/abstract/document/10620094 (accessed on 19 February 2025).

 doi:10.20944/preprints202504.1401.v1

5. Chauveau, A. *Nouvelles Recherches Expérimentales sur les Mouvements et les Bruits Normaux du Cœur*; J.-B. Baillère: Paris, France, 1856.
6. IoT-Powered Predictive Maintenance Framework for ICU Ventilators. Available online: https://ieeexplore.ieee.org/abstract/document/10620162 (accessed on 19 February 2025).
7. Atanasoski, V.; Maneski, L.P.; Ivanović, M.D. SimEMG Database as a Tool for Testing the Preservation of Diagnostic ECG-Signal Features upon the Electromyographic Noise Removal.
8. Reynier, P. *Des Nerfs du Coeur: Anatomie et Physiologie*; J.-B. Ballière: Paris, France, 1880.
9. Qin, Y.; et al. A Novel Adaptive Filter with a Heart-Rate-Based Reference Signal for Esophageal Pressure Signal Denoising. *J. Clin. Monit. Comput.* **2024**. https://doi.org/10.1007/s10877-023-01116-z.
10. Atanasoski, V.; et al. A Morphology-Preserving Algorithm for Denoising of EMG-Contaminated ECG Signals. *IEEE Open J. Eng. Med. Biol.* **2024**, *5*, 296–305. https://doi.org/10.1109/OJEMB.2024.3380352.
11. Revach, G.; Locher, T.; Shlezinger, N.; van Sloun, R.J.G.; Vullings, R. HKF: Hierarchical Kalman Filtering with Online Learned Evolution Priors for Adaptive ECG Denoising. *arXiv* **2023**, arXiv:2210.12807. Available online: http://arxiv.org/abs/2210.12807 (accessed on 10 March 2024).
12. Mvuh, F.L.; Ebode Ko'a, C.O.V.; Bodo, B. Multichannel High Noise Level ECG Denoising Based on Adversarial Deep Learning. *Sci. Rep.* **2024**, *14*, 801. https://doi.org/10.1038/s41598-023-50334-7.
13. Occhipinti, E.; et al. In-Ear ECG Signal Enhancement with Denoising Convolutional Autoencoders. *arXiv* **2024**, arXiv:2409.05891. https://doi.org/10.48550/arXiv.2409.05891.
14. Wang, K.-C.; Liu, K.-C.; Peng, S.-Y.; Tsao, Y. ECG Artifact Removal from Single-Channel Surface EMG Using Fully Convolutional Networks. *arXiv* **2022**, arXiv:2210.13271. https://doi.org/10.48550/arXiv.2210.13271.
15. Liu, Y.-T.; Wang, K.-C.; Liu, K.-C.; Peng, S.-Y.; Tsao, Y. SDEMG: Score-Based Diffusion Model for Surface Electromyographic Signal Denoising. *arXiv* **2024**, arXiv:2402.03808. https://doi.org/10.48550/arXiv.2402.03808.
16. Crabbé, J.; Huynh, N.; Stanczuk, J.; van der Schaar, M. Time Series Diffusion in the Frequency Domain. *arXiv* **2024**, arXiv:2402.05933. https://doi.org/10.48550/arXiv.2402.05933.
17. Saleem, S.; Khandoker, A.H.; Alkhodari, M.; Hadjileontiadis, L.J.; Jelinek, H.F. A Two-Step Pre-Processing Tool to Remove Gaussian and Ectopic Noise for Heart Rate Variability Analysis. *Sci. Rep.* **2022**, *12*, 18396. https://doi.org/10.1038/s41598-022-21776-2.
18. Moody, G.B.; Mark, R.G. MIT-BIH Arrhythmia Database. *physionet.org* **1992**. https://doi.org/10.13026/C2F305.
19. Preprocessing and Denoising Techniques for Electrocardiography and Magnetocardiography: A Review. Available online: https://www.mdpi.com/2306-5354/11/11/1109 (accessed on 25 November 2024).
20. Hu, K.-Y.; Wang, J.; Cheng, Y.; Yang, C. Adaptive Filtering and Smoothing Algorithm Based on Variable Structure Interactive Multiple Model. *Sci. Rep.* **2023**, *13*, 12993. https://doi.org/10.1038/s41598-023-39075-9.
21. Yang, X.; Wang, W. Chaotic Signal Denoising Based on Energy Selection TQWT and Adaptive SVD. *Sci. Rep.* **2023**, *13*, 18873. https://doi.org/10.1038/s41598-023-45811-y.
22. Tong, S.; Yu, D.; Li, X.; Wang, L.; Wang, L. Research on ECG Signal Denoising Based on EM-UKF Algorithm. In *Proceedings of the 2024 9th International Conference on Multimedia Systems and Signal Processing (ICMSSP)*, New York, NY, USA, October 2024; pp. 18–23. https://doi.org/10.1145/3690063.3690067.
23. Improved Multi-Layer Wavelet Transform and Blind Source Separation Based ECG Artifacts Removal Algorithm from the sEMG Signal: In the Case of Upper Limbs. Available online: https://www.frontiersin.org/articles/10.3389/fbioe.2024.1367929/full (accessed on 25 November 2024).
24. Sameni, R.; Shamsollahi, M.B.; Jutten, C.; Clifford, G.D. A Nonlinear Bayesian Filtering Framework for ECG Denoising. *IEEE Trans. Biomed. Eng.* **2007**, *54*, 2172–2185. https://doi.org/10.1109/TBME.2007.897817.
25. Dataset for Multi-Channel Surface Electromyography (sEMG) Signals of Hand Gestures. Available online: https://data.mendeley.com/datasets/ckwc76xr2z/2 (accessed on 25 November 2024).
26. Denoising of Blasting Vibration Signals Based on CEEMDAN-ICA Algorithm. Available online: https://www.nature.com/articles/s41598-023-47755-9 (accessed on 10 March 2024).
27. High-Density Surface EMG Denoising Using Independent Vector Analysis. Available online: https://ieeexplore.ieee.org/document/9064821 (accessed on 19 February 2025).
28. Radware Bot Manager Captcha. Available online: https://ieeexplore.ieee.org (accessed on 19 February 2025).
29. Komorowski, D.; Mika, B.; Kaczmarek, P. A New Approach to Preprocessing of EMG Signal to Assess the Correctness of Muscle Condition. *Sci. Pap. Silesian Univ. Technol. Organ. Manag. Ser.* **2023**, *186*, 217–238. https://doi.org/10.29119/1641-3466.2023.186.17.
30. Ponnada, S.; Kuan Tak, T.; Kshirsagar, P.R.; Srinivasa Rao, P.; Dayal, A. Expanding Applications of TinyML in Versatile Assistive Devices: From Navigation Assistance to Health Monitoring Sys-

 doi:10.20944/preprints202504.1401.v1

tem Using Optimized NASNet-XGBoost Transfer Learning. *IEEE Access* **2024**, *12*, 168328–168338. https://doi.org/10.1109/ACCESS.2024.3496791.

31. Noise Removal in Single-Lead Capacitive ECG with Adaptive Filtering and Singular Value Decomposition. Available online: https://ieeexplore.ieee.org/abstract/document/10714420 (accessed on 25 November 2024).
32. Zhang, Z.; Ye, Y.; Luo, B.; Chen, G.; Wu, M. Investigation of Microseismic Signal Denoising Using an Improved Wavelet Adaptive Thresholding Method. *Sci. Rep.* **2022**, *12*, 22186. https://doi.org/10.1038/s41598-022-26576-2.
33. Farag, M.M. A Tiny Matched Filter-Based CNN for Inter-Patient ECG Classification and Arrhythmia Detection at the Edge. *Sensors* **2023**, *23*, 31365. https://doi.org/10.3390/s23031365.
34. Kim, J.; Kim, E.; Kyung, Y.; Ko, H. A Study on ECG Monitoring Embedded Systems. In *Proceedings of the 2022 13th International Conference on Information and Communication Technology Convergence (ICTC)*, Jeju, Korea, October 2022; pp. 1671–1673. https://doi.org/10.1109/ICTC55196.2022.9952978.
35. Busia, P.; Scrugli, M.A.; Jung, V.J.-B.; Benini, L.; Meloni, P. A Tiny Transformer for Low-Power Arrhythmia Classification on Microcontrollers. *IEEE Trans. Biomed. Circuits Syst.* **2024**, 1–11. https://doi.org/10.1109/TBCAS.2024.3401858.
36. Ibrahim, M.F.R.; Alkanat, T.; Meijer, M.; Schlaefer, A.; Stelldinger, P. End-to-End Multi-Modal Tiny-CNN for Cardiovascular Monitoring on Sensor Patches. In *Proceedings of PerCom 2024*, Biarritz, France, March 2024; p. 24. https://doi.org/10.1109/PerCom59722.2024.10494450.
37. Ficco, M.; Guerriero, A.; Milite, E.; Palmieri, F.; Pietrantuono, R.; Russo, S. Federated Learning for IoT Devices: Enhancing TinyML with On-Board Training. *Inf. Fusion* **2024**, *104*, 102189. https://doi.org/10.1016/j.inffus.2023.102189.
38. IEEE Xplore Full-Text PDF. Available online: https://ieeexplore.ieee.org/stamp/stamp.jsp?arnumber=10496107 (accessed on 6 January 2025).
39. Riillo, F.; et al. Optimization of EMG-Based Hand Gesture Recognition: Supervised vs. Unsupervised Data Preprocessing on Healthy Subjects and Transradial Amputees. *Biomed. Signal Process. Control* **2014**, *14*, 117–125. https://doi.org/10.1016/j.bspc.2014.07.007.
40. Bashford, J.; et al. Preprocessing Surface EMG Data Removes Voluntary Muscle Activity and Enhances SPiQE Fasciculation Analysis. *Clin. Neurophysiol.* **2020**, *131*, 265–273. https://doi.org/10.1016/j.clinph.2019.09.015.
41. Hayajneh, A.M.; Aldalahmeh, S.; Zaidi, S.A.R.; McLernon, D.; Obeidollah, H.; Alsakarnah, R. Channel State Information Based Device-Free Wireless Sensing for IoT Devices Employing TinyML. In *Proceedings of the 2022 4th IEEE Middle East and North Africa Communications Conference (MENACOMM)*, Amman, Jordan, December 2022; pp. 215–222. https://doi.org/10.1109/MENACOMM57252.2022.9998267.
42. Riillo, F.; et al. Optimization of EMG-Based Hand Gesture Recognition: Supervised vs. Unsupervised Data Preprocessing on Healthy Subjects and Transradial Amputees. *Biomed. Signal Process. Control* **2014**, *14*, 117–125. https://doi.org/10.1016/j.bspc.2014.07.007.